HHS Public Access

Author manuscript

Hum Brain Mapp. Author manuscript; available in PMC 2017 February 01.

Published in final edited form as:

Hum Brain Mapp. 2016 February ; 37(2): 745–755. doi:10.1002/hbm.23063.

Hemodynamic Response Function Abnormalities in Schizophrenia During a Multisensory Detection Task

Faith M. Hanlon[1], **Nicholas A. Shaff**[1], **Andrew B. Dodd**[1], **Josef M. Ling**[1], **Juan R. Bustillo**[2,3], **Christopher C. Abbott**[2], **Shannon F. Stromberg**[2], **Swala Abrams**[2], **Denise S. Lin**[2], and **Andrew R. Mayer**[1,2,4,5,*]

[1]The Mind Research Network/Lovelace Biomedical and Environmental Research Institute, Albuquerque, NM 87106 USA

[2]Department of Psychiatry, University of New Mexico School of Medicine, Albuquerque, NM 87131 USA

[3]Department of Neuroscience, University of New Mexico School of Medicine, Albuquerque, NM 87131 USA

[4]Department of Neurology, University of New Mexico School of Medicine, Albuquerque, NM 87131 USA

[5]Department of Psychology, University of New Mexico, Albuquerque, NM 87131 USA

Abstract

Functional magnetic resonance imaging (fMRI) of the blood oxygen level dependent (BOLD) response has commonly been used to investigate the neuropathology underlying cognitive and sensory deficits in patients with schizophrenia (SP) by examining the positive phase of the BOLD response, assuming a fixed shape for the hemodynamic response function (HRF). However, the individual phases (positive and post-stimulus undershoot (PSU)) of the HRF may be differentially affected by a variety of underlying pathologies. The current experiment used a multisensory detection task with a rapid event-related fMRI paradigm to investigate both the positive and PSU phases of the HRF in SP and healthy controls (HC). Behavioral results indicated no significant group differences during task performance. Analyses that examined the shape of the HRF indicated two distinct group differences. First, SP exhibited a reduced and/or prolonged PSU following normal task-related positive BOLD activation in secondary auditory and visual sensory areas relative to HC. Second, SP did not show task-induced deactivation in the anterior node of the default-mode network (aDMN) relative to HC. In contrast, when performing traditional analyses that focus on the positive phase, there were no group differences. Interestingly, the magnitude of the PSU in secondary auditory and visual areas was positively associated with the magnitude of task-induced deactivation within the aDMN, suggesting a possible common neural mechanism underlying both of these abnormalities (failure in neural inhibition). Results are consistent with recent views that separate neural processes underlie the two phases of the HRF and that they are differentially affected in SP.

[*]Corresponding author: Andrew Mayer, Ph.D., The Mind Research Network, Pete & Nancy Domenici Hall, 1101 Yale Blvd. NE, Albuquerque, NM 87106 USA; Tel: 505-272-0769; Fax: 505-272-8002; amayer@mrn.org.

Keywords

fMRI; post-stimulus undershoot; inhibition; blood oxygen level dependent response; auditory; visual

Introduction

Schizophrenia is a complex disorder, marked by generalized cognitive and sensory deficits and psychiatric symptoms. Functional magnetic resonance imaging (fMRI) of the blood oxygen level dependent (BOLD) response has commonly been used to investigate the underlying neuropathology associated with these deficits (Ragland et al., 2007). However, the vast majority of studies have only examined the positive phase of the hemodynamic response function (HRF). Importantly there is emerging evidence that multiple aspects of the HRF may be abnormal in patients with schizophrenia (SP; Dyckman et al., 2011; Mayer et al., 2013), and that the individual phases of the HRF are affected by different underlying pathologies (Handwerker et al., 2012).

Although the exact mechanisms of neurovascular coupling remain debated (see Attwell et al., 2010; Petzold and Murthy, 2011 for reviews), glutamate-mediated signaling in neurons and astrocytes triggers vasoactive signals to arterioles and capillaries, resulting in dilation of upstream arterial vessels and a subsequent increase in cerebral blood flow (CBF). CBF increases to a larger degree than the cerebral metabolic rate of oxygen utilization ($CMRO_2$), which alters the ratio of oxyhemoglobin (i.e., increased) to deoxyhemoglobin relative to the baseline state (Fox and Raichle, 1986). The altered ratio of oxy- to deoxyhemoglobin is the primary driver of the positive phase of the BOLD response, which peaks approximately 4 to 6 seconds post-stimulus onset (Buxton, 2012; Buxton et al., 2004; Kim and Ogawa, 2012).

However, the canonical HRF also includes the post-stimulus undershoot (PSU), which negatively peaks approximately 10 to 14 seconds after the stimulus ends (Buxton, 2012). The hemodynamic hypothesis posits that the PSU results from hypo-perfusion in CBF and/or a slow return of cerebral blood volume (CBV; balloon model) to baseline levels (Buxton et al., 1998; Buxton et al., 2004; Chen and Pike, 2009). In contrast, other theories suggest that increased metabolic demands ($CMRO_2$) following cellular signaling represent the primary contribution to the PSU (Hua et al., 2011; Lu et al., 2004; Schroeter et al., 2006). Finally, some have suggested that inhibitory neural activity underlying the PSU is distinct from excitatory activity underlying the positive HRF phase (Mullinger et al., 2013; Sadaghiani et al., 2009). In addition to these neural factors, the magnitude of the PSU response may also be influenced by stimulus duration and spatial proximity to source of activation (Harshbarger and Song, 2008; van Zijl et al., 2012).

In the vast majority of psychiatric research, the BOLD response is typically estimated by a single parameter (a beta weight) following convolution of a canonical HRF (e.g., a gamma variate or a double gamma variate function) with known experimental conditions (e.g., design matrix). Such modeling may mask and/or accentuate pathologies that influence only one aspect of the BOLD response (either the positive phase or the PSU). This is particularly problematic in SP, where the HRF may be affected by disease-related neuronal pathology

including cortical volume loss (De et al., 2012), altered glutamate/glutamine and GABA concentrations (Poels et al., 2014; Taylor and Tso, 2014), abnormal glucose metabolism (Harris et al., 2013), and/or vascular differences altering blood flow/volume (Kindler et al., 2015; Liu et al., 2012; Peruzzo et al., 2011; Zhu et al., 2015). Alternatively, changes to the HRF in SP may also partially result from secondary disease characteristics including increased smoking (Friedman et al., 2008; Leyba et al., 2008) and antipsychotic medication effects (Abbott et al., 2013; Roder et al., 2010).

The few studies explicitly examining the timing and/or shape of the HRF in SP have reported a delay during a visual oddball task (Ford et al., 2005) or differences in its onset transient during a working memory task (Fox et al., 2005). Others have observed differences in both the timing and shape of the HRF. Mayer et al. (2013) reported that patients' auditory HRF required several additional seconds to return to baseline and included a reduced PSU using qualitative metrics during a sensory gating task. In another inhibitory task, Dyckman et al. (2011) found that the HRF for SP had both a delayed time-to-peak and a prolonged positive phase during antisaccades but not prosaccades. Importantly, in both studies (Dyckman et al., 2011; Mayer et al., 2013) the amplitude of the positive phase of the HRF was similar between groups, potentially leading to a misinterpretation of results if only this aspect of the HRF was to be examined.

The current experiment used a multisensory detection task in conjunction with a rapid event-related fMRI paradigm to investigate abnormalities in the shape of the HRF in SP. The event-related design provides a more accurate estimation of the HRF (D'Esposito et al., 1999). A simple detection task should reduce behavioral performance confounds (i.e., reduced accuracy or slower responses) typically observed in SP (Van Snellenberg et al., 2006) that can also alter the shape of the HRF (i.e., delayed HRF due to delayed response time). Based on our previous observations, we predicted that SP would be associated with a reduced PSU in task-related areas in conjunction with normal activation for the positive phase of the BOLD response (Mayer et al., 2013).

Materials and Methods

Participants

Thirty-five SP and thirty-five age, sex and education-matched HC participated in the current study. Two patients and one HC were identified as having excessive (greater than three standard deviations [SD]) motion (frame-wise displacement) within their cohort on two of six parameters and were subsequently eliminated from further analyses (Mayer et al., 2007). None of the participants were excluded due to poor task performance (accuracy: greater than 5 misses; reaction time: outlier greater than three SD relative to cohort). This left a final dataset of 33 SP (27 males; 38.09±13.66 years old; 12.61±1.77 years of education) and 34 HC (28 males; 37.50±13.35 years old; 12.74±1.83 years of education). All participants provided informed consent according to institutional guidelines at the University of New Mexico.

Inclusion criteria for SP included a diagnosis of schizophrenia or schizoaffective disorder by board certified psychiatrists based on the Structured Clinical Interview for DSM-IV-TR

(SCID) and age of 18 to 65 years. All of the patients were taking stable doses of antipsychotic medications (28/33 were taking atypical antipsychotic medication) and olanzapine equivalency scores were calculated to estimate medication load (Gardner et al., 2010). Exclusion criteria for both patients and HC included a history of neurological disorder, head trauma with loss of consciousness greater than five minutes, active substance dependence or abuse (except for nicotine) within the past year, lifetime history of dependence or use within the last 12 months of hallucinogens, amphetamines or cocaine, or intellectual disability. Additional exclusion criteria for HC included history of a psychotic disorder in a first-degree relative, a current or past psychiatric disorder (with the exception of one lifetime depressive episode), depression or antidepressant use within the last six months, or lifetime antidepressant use of more than one year. Participants abstained from smoking and caffeine intake for at least one hour before imaging.

Clinical Assessment

All participants completed the Wechsler Test of Adult Reading (WTAR) as an estimate of pre-morbid intelligence (Wechsler, 2001). Patient clinical assessments included: Positive and Negative Syndrome Scale (PANSS; Kay et al., 1987), Calgary Depression Scale (Addington et al., 1993), Fagerstrom Test for Nicotine Dependence (FTND; Heatherton et al., 1991), a modified version of the Simpson Angus Scale for parkinsonism (SAS; Simpson and Angus, 1970), Abnormal Involuntary Movements Scale (AIMS; Guy, 1976) for tardive dyskinesia, Barnes Akathisia Scale (BAS; Barnes, 1989), and urine drug screening. Everyday functioning was measured with the UCSD Performance Based Skills Assessment (UPSA-2; Patterson et al., 2001).

Task

All participants completed a multisensory detection task (Figure 1A) while undergoing fMRI data collection on a 3.0 Tesla Siemens Trio Tim scanner using a 12-channel head coil. Presentation software (Neurobehavioral Systems) was used for task stimulus presentation, synchronization of stimulus events with the MRI scanner, and recording of response times. Additional foam padding was used around the head to limit head motion within the head coil. The target stimuli consisted of a simultaneously presented blue box (visual angle = 4.3 × 6.5°) and auditory (2000 Hz re-sampled with a 10 ms linear ramp) tone for a 300 ms duration (Figure 1A). Participants pressed a button with their right index finger to indicate target detection (35 total trials). The baseline stimuli was a white visual fixation cross (visual angle = 0.9°) on a black background. The duration of the inter-trial interval varied from 4 to 8 seconds to prevent the development of temporal expectations, non-linear summing of the hemodynamic response (Glover, 1999) and to allow for the best sampling of the hemodynamic response (Burock et al., 1998). Auditory and visual stimuli were also time-locked to the repetition time (TR) to facilitate deconvolution analyses.

MR Imaging

High resolution 5-echo multi-echo Magnetization Prepared Rapid Acquisition Gradient Echo (MPRAGE) T_1 [repetition time (TR) = 2.53 s, 7° flip angle, echo times (TE) = 1.64, 3.5, 5.36, 7.22, 9.08 ms, number of excitations (NEX) = 1, slice thickness = 1 mm, field of view (FOV) = 256 mm, resolution = 256 × 256] were collected for structural images. Echo-

planar images were collected using a single-shot, gradient-echo echoplanar pulse sequence [TR = 2000 ms; TE = 29 ms; flip angle = 75°; FOV = 240 mm; matrix size = 64 × 64]. Thirty-three contiguous 3.5-mm thick sagittal slices with a gap factor of 1.05 mm were selected to provide whole-brain coverage (voxel size: 3.75 × 3.75 × 4.55 mm). The first three images of the run were eliminated to account for T_1 equilibrium effects, resulting in a total of 114 images for the final analyses.

Image Processing and Statistical Analyses

Functional images were generated using Analysis of Functional NeuroImages (AFNI) software package (Cox, 1996). Time series images were de-spiked, temporally interpolated to correct for slice-time acquisition differences, and spatially registered in both two- and three-dimensional space to the second EPI image of the run to minimize effects of head motion. Anatomical and functional images were then converted to a standard stereotaxic coordinate space (Talairach and Tournoux, 1988), interpolated to volumes with 3 mm^3 voxels, and blurred with a 6 mm full width at half maximum (FWHM) Gaussian kernel.

A deconvolution analysis was then performed on a voxel-wise basis to generate an HRF for the multisensory-motor stimuli using the following equation:

$$\begin{aligned} Y(n) &= \beta_0 + \beta_1 n + h(0)f(n) + h(1)f(n-1) + \ldots + h(9)f(n-9) + e(n) \\ &= \beta_0 + \beta_1 n + \sum_{i=0}^{9} h(i)f(n-i) + e(n) \end{aligned} \quad \text{(Eq. 1)}$$

where the observed signal (*Y*) at each time-point (*n*) is defined as a linear combination of a constant term (β_0), linear (β_1) and other higher-order polynomial terms, and the experimental condition (denoted by the vector *h*) multiplied by a binary vector (*f*) indicating whether the experimental condition occurred on the current and/or previous nine images. The solution is optimized by minimizing the ordinary sum of squares of the residual error term, represented by *e(n)*. In addition, 12 motion regressors (6 motion parameters and their derivatives) were included in the deconvolution analyses to reduce the impact of head motion on patterns of functional activation. Each HRF was derived relative to the baseline state (visual fixation plus baseline gradient noise) and based on the first 20 seconds (10 images) post-stimulus onset. Resulting beta coefficients were normalized by dividing by the model intercept to form an estimate of percent signal change (PSC).

A 2 × 10 (Group x Time) voxel-wise linear mixed-effect ANCOVA was used to examine group differences in the shape of the HRF with subjects as a random effect. An autoregressive model (*AR*(1)) was used for the covariance matrix to capture time-series dependencies (Box et al., 1994). In this analytic framework, a Group x Time interaction indicates regions where the shape of the HRF systematically differed across groups. The main effect of time represents regions exhibiting systematic variability across the different beta coefficients, and is deemed of insufficient interest (i.e., a high-rate of significant effects secondary to variability) for follow-up analyses.

Voxel-wise independent groups t-tests were also conducted to compare activation for each group during the peak positive BOLD phase (images occurring 4 – 8 s post-stimulus onset;

average PSC from the 3rd and 4th TR) and the peak PSU (images occurring 10 – 14 s post-stimulus onset; average PSC from the 6th and 7th TR) to represent a more standard analytic approach. Within-subject comparisons (SP and HC separately; see Supplemental Results) were also used to aid in the identification of neuronal networks positively or negatively differentiated from baseline (i.e., two sided t-tests) for both the peak positive BOLD phase and the peak PSU. To operationally differentiate a PSU from task-induced deactivation, we stipulated that the PSU had to occur after an initial positive BOLD response to stimuli. A significance threshold corresponding to $p < 0.005$ was applied in combination with a minimum cluster size threshold of 1152 microliters (18 native voxels) to minimize false positives for all comparisons. This resulted in a corrected p value of 0.05 based on 10,000 Monte Carlo simulations (Forman et al., 1995).

Linear regressions were used to evaluate the relationships between observed HRF abnormalities and either 1) clinical measures or 2) motor side-effects in SP only. The five independent variables used for the analyses of clinical measures included 1) UPSA-2 total score, 2) PANSS Negative symptoms score, 3) PANSS Positive symptoms score, 4) Olanzapine equivalence score, and 5) FTND scores. The independent variables for regressions examining motor side-effects were the 1) AIMS, 2) BAS and 3) SAS.

Results

Demographics and Clinical Measures

Independent samples t-tests indicated that there were no significant differences between SP and HC ($p > 0.10$) on major demographic variables (age and education). There was no significant difference ($p > 0.10$) in estimated levels of premorbid intellectual functioning (WTAR). A compilation of all major clinical indices is presented in Table I.

Behavioral Data

Accuracy was near ceiling for both SP (98.6±3.0%) and HC (99.7±0.9%) samples. As a result these data were not analyzed further. Response time data were non-normally distributed, with results from Mann-Whitney U test indicating no group differences ($p > 0.10$) in response time (Figure 1B; SP: 364.1±127.8 ms; HC: 318.8±123.2 ms).

Functional Imaging Data Quality Assurance

Two MANOVAs were conducted to investigate any possible group differences in head motion (rotational and translational displacements) that might confound interpretation of fMRI data. The multivariate effect of group was not significant for translational or rotational motion ($p > 0.10$). However, some univariate effects of motion were significant (pitch: $p = 0.024$) or at trend level (roll: $p = 0.098$; yaw: $p = 0.063$; y-axis: $p= 0.093$), with moderate effect sizes (Cohen's D range from 0.32 to 0.56) across all 6 parameters. Therefore, mean framewise displacement was used as a covariate in all further analyses as a conservative measure.

fMRI Analyses Examining HRF Shape

A 2 × 10 [Group x Time] (0 to 20 s post-stimulus onset) linear mixed effects whole-brain ANCOVA was performed next to examine group differences in the shape of the HRF. The main effect of group was not significant following correction for false positives. However, there were several regions (Figure 2A) that demonstrated a significant Group x Time interaction. These included the anterior cingulate gyrus (ACC)/medial prefrontal cortex, comprising the anterior node of the default mode network (aDMN; BAs b. 10/24/32, r. 9); the right secondary auditory cortex including superior temporal gyrus (STG), insula, and pre-/post-central gyrus (BAs 4/6/13/22/43); and the precuneus, cuneus and posterior cingulate gyrus (BAs b. 7/18/30/31, r. 19).

Follow-up simple effect testing was then conducted for each region at each time-point to determine the direction of the group effect. Results indicated that HC showed significantly decreased activation in the aDMN (8 – 10 s post-stimulus onset: $t_{65} = -2.19$, $p = .032$; 10 – 12 s: $t_{65} = -2.86$, $p = .006$; 12 – 14 s: $t_{55.8} = -2.86$, $p = .006$; 14 – 16 s: $t_{65} = -2.34$, $p = .022$) relative to no deviation from baseline for SP (Figure 2B). In contrast, SP showed a significantly reduced PSU for the right secondary auditory cortex (8 – 10 s: $t_{58.5} = -2.77$, $p = .007$) relative to HC. Finally, SP showed a prolonged PSU for the precuneus (16 – 18 s: $t_{65} = 2.01$, $p = .049$) compared to HC.

Next linear regressions were performed to determine if activity within secondary auditory cortex or precuneus was related to deactivation within the aDMN across both groups of subjects. Average gray matter PSC for the PSU was used as a covariate to control for individual differences in global brain activity. Results indicated a significant relationship between the aDMN and secondary auditory cortex (Figure 2C; unstandardized $\beta = 0.564$, $t_{63} = 7.51$, $p < 0.01$), as well as between the aDMN and precuneus (unstandardized $\beta = 0.170$, $t_{63} = 2.37$, $p = 0.021$). Results remained significant (all p's < 0.05) even when subjects with higher activation/deactivation values were removed.

Voxel-wise ANCOVAs were also performed to assess more traditional analyses for comparing group differences in the positive phase (4 to 8 seconds post-stimulus onset) or the PSU (10 to 14 seconds) of the HRF. However, results for both analyses were not significant following correction for multiple comparisons. Results from within-subject analyses comparing the positive phase and PSU images to baseline for each separately are displayed in Supplemental Results and Figure S1. The task resulted in the expected patterns of activation across both groups.

Activation and Clinical Interactions

Linear regression evaluated the relationship between HRF abnormalities and either 1) clinical measures or 2) potential motor side-effects in SP only. Only PSC data from time-points exhibiting significant simple effects (average time-points for the aDMN) from the deconstruction of the Group x Time interaction were used as the dependent variables in these analyses, and results were not corrected for multiple comparisons given the exploratory nature of the analyses. The overall model was not significant in any of the six regressions (all p's > 0.10). Among univariate effects, only the relationship between degree

of deactivation in secondary auditory cortex and total UPSA-2 score was significant (β = −0.522, t = −2.61, p = 0.015), with higher levels of everyday functioning predictive of more deactivation in the area.

Discussion

The majority of previous investigations in SP have assumed a fixed shape for the HRF during comparisons to HC, an assumption which may not be valid due to differences in neurovascular coupling and other disease-related pathologies (Dyckman et al., 2011; Handwerker et al., 2012; Mayer et al., 2013). Behavioral results from the current study confirmed expectations of non-significant group differences in response time or task accuracy during multisensory stimuli detection. Analyses examining the shape of the HRF indicated two patterns of abnormalities involving 1) a reduced/prolonged PSU following task-related positive BOLD activation in secondary unisensory cortex and 2) a lack of task-induced deactivation in the aDMN. Importantly, additional analyses suggested that these two patterns of BOLD abnormalities were related, suggesting deficits in inhibition as a common underlying mechanism. In contrast, there were no group differences during more traditional analyses that specifically focused on the positive phase of the HRF.

We previously observed differences in the HRF shape between SP and HC in auditory cortex during a sensory gating task (Mayer et al., 2013), while others have reported differences in HRF shape in bilateral frontal eye fields during antisaccades (Dyckman et al., 2011). In the current experiment, SP exhibited a reduced/prolonged PSU in bilateral secondary visual areas (precuneus and cuneus) and reduced PSU in right secondary auditory cortex during a multisensory (auditory and visual) detection task. Positive BOLD activation was observed in the HRF of these regions in both groups of participants as well (Figure 2B), with supplemental analyses focusing on the magnitude of the positive phase indicating no significant group differences. The magnitude of the PSU in secondary auditory cortex was also associated with decreased performance on a test of everyday functioning. Thus, PSU abnormalities may be both more sensitive to certain kinds of neural deficits than the positive phase and have some specificity in terms of association with real-world activities. Interestingly, the time ranges in which group differences in these sensory areas were found (8 – 10 s and 16 – 18 s) were not included in our analyses of either the positive or PSU phases, reaffirming the importance of examining the entire HRF. Previous studies have indicated hemodynamic abnormalities when modeling the shape of the HRF within visual and auditory unisensory cortex in SP (Dyck et al., 2014; Gaebler et al., 2015), indicating that abnormalities are not limited to the PSU.

Collectively, current results are consistent with the view that separate neural processes underlie the two phases of the HRF (Haigh et al., 2015; Mullinger et al., 2013; Sadaghiani et al., 2009), and that they are differentially affected in SP (Figure S1). The PSU was classically thought to originate from passive differences in vascular reactivity (balloon model; Buxton et al., 1998; Buxton et al., 2004; Chen and Pike, 2009), with more recent theories also suggesting a contribution from increased metabolic demands ($CMRO_2$; Hua et al., 2011; Lu et al., 2004; Schroeter et al., 2006). In line with both theories, there are several studies that have indicated abnormal CBF (Kindler et al., 2015; Zhu et al., 2015) and

glucose metabolic dysfunction (Buchsbaum et al., 2007; Fujimoto et al., 2007) in SP in similar regions that showed HRF abnormalities in the current study (i.e., unisensory cortex and ACC). Alternatively, structural or neurochemical abnormalities could also have contributed to the reduced PSU observed in the current study. For example, the anterior and posterior insula (Shepherd et al., 2012) and STG (Vita et al., 2012) exhibit volume loss in SP, and abnormal levels of glutamate/glutamine/GABA have been reported in SP (Poels et al., 2014; Taylor and Tso, 2014). The former affects perfusion whereas glutamate and GABA directly affect the shape of the HRF, potentially differentially in HC and SP (Falkenberg et al., 2014; Muthukumaraswamy et al., 2012).

The second major finding of the study was that SP did not exhibit task-induced deactivation of aDMN relative to HC. The aDMN has been linked with monitoring and mentalizing of our own and others' psychological states (Broyd et al., 2009). Previous studies reported reduced task-induced deactivation during more complex tasks in SP (Landin-Romero et al., 2015; Mothersill et al., 2014; Nygard et al., 2012; Pomarol-Clotet et al., 2008), although contrary findings of increased DMN task-induced deactivation for SP have also been observed (Harrison et al., 2007; Mannell et al., 2010). Disparities in the degree of task-induced deactivation across studies may result from the type of task/cognitive load, anterior vs. posterior regions of the DMN, or performance of participants on tasks (Harrison et al., 2007; Mannell et al., 2010; McKiernan et al., 2003; Nygard et al., 2012; Pomarol-Clotet et al., 2008).

Finally, the magnitude of the PSU in secondary auditory and visual areas was positively associated with the magnitude of task-induced deactivation within the aDMN, suggesting that there may be a common neural mechanism underlying both of these abnormalities, such as neural inhibition. Specifically, negative BOLD responses may result from inhibitory neural activity and concomitant changes in CBF and CBV that are opposite of the neurophysiology occurring during the positive phase (Boorman et al., 2010; Devor et al., 2007; Mullinger et al., 2013). Invasive recordings in animal models suggest that neuronal suppression in deep cortical layers precedes the negative BOLD response as a result of arteriolar vasoconstriction (decreases in CBF and CBV) and a subsequent increase in local deoxyhemoglobin (Boorman et al., 2010; Devor et al., 2007; Shmuel et al., 2006). For example, in primate visual areas, using simultaneous fMRI and electrophysiological recordings, a trial-by-trial analysis found a tight coupling between negative BOLD response and decreased neural activity (Shmuel et al., 2006). In HC, negative BOLD responses have been observed during transcallosal motor inhibition (McGregor et al., 2014), when information from one sensory modality is actively suppressed (Johnson and Zatorre, 2006; Mayer et al., 2009) and when participants switch from passive to attentionally demanding states within the DMN (McKiernan et al., 2003).

Similarly, recent theories suggest that the PSU may actually represent neural inhibition following excitation. Invasive electrophysiological recordings in primate visual areas show a below baseline decrease in neural activity for up to 10 s following excitatory activity (Shmuel et al., 2006). Moreover, there is also a relationship between the amplitude and direction of the PSU and post-stimulus event-related synchronization (PERS), a rebound in the alpha and/or beta frequencies that occurs following motor tasks, sensorimotor, or visual

stimulation and serves as a marker of functional inhibition (Jurkiewicz et al., 2006; Klimesch et al., 2007; Stevenson et al., 2011). Specifically, both BOLD and CBF undershoots in primary sensorimotor cortices were found in trials with high PERS mu power, as well as reduced $CMRO_2$ compared with baseline following median nerve stimulation (Mullinger et al., 2013).

Thus, current findings of abnormal negative BOLD responses, for both the PSU in task-related areas and task-induced deactivation in aDMN, may reflect a more global mechanism of inhibitory failure for SP. Previous studies have described GABA abnormalities in SP using both post-mortem tissue analyses and magnetic resonance spectroscopy (Rowland et al., 2013; Rowland et al., 2015; Taylor and Tso, 2014). Similarly, transcranial magnetic stimulation (TMS) studies have also reported intracortical inhibitory deficits in the motor cortex of SP. Finally, inhibitory deficits have been observed in SP across a variety (e.g., anti-saccade, auditory and sensorimotor gating) of tasks (Braff et al., 2001; McDowell and Clementz, 2001). These findings suggest that inhibitory deficits are a fundamental pathophysiological mechanism in schizophrenia and may be related to decreases in inhibitory interneurons (Lara, 2002).

There are several limitations to the current study. First, although we examined the impact of medication use, motor-side effects and smoking status in regards to our findings, we cannot entirely rule-out their effects on neurovascular coupling, the vasculature and hence the HRF (Friedman et al., 2008; Leyba et al., 2008; Roder et al., 2010). For example, certain antipsychotic medications (e.g., olanzapine and risperidone) result in cardiovascular abnormalities in both pre-clinical and human studies (Aboul-Fotouh and Elgayar, 2013; Leung et al., 2012; Leung et al., 2014), which may directly affect the HRF (Abbott et al., 2013; Roder et al., 2010). Similarly, HRF may also be influenced by other disease-related changes to perfusion, metabolism, structure volume loss, neurochemical, or a combination of any of these factors, all of which would impact on current findings. Future studies that employ multimodal neuroimaging techniques could disambiguate these various potential etiologies.

Second, previous findings suggest that the two key assumptions of deconvolution (additive in a linear fashion and time invariant) are generally met for the HRF as long as a minimum inter-trial interval of 4 seconds is maintained (Glover, 1999). However, these data were primarily based on assumptions from a modified balloon model, which emphasizes vascular over post-excitatory neural contributions to the HRF. Importantly, our minimum inter-trial interval was 4 seconds, with the majority of trials occurring at 6 or 8 second intervals, which should decrease the likelihood of non-linear summing. Third, we did not attempt to explicitly model the deconvolved HRF with a gamma variate or a double gamma variate function as has been previously done (Bellgowan et al., 2003; Mayer et al., 2014; Thompson et al., 2014). Modeling 8 free parameters (i.e., a double gamma variate function) based on 10 data points (i.e., our measured HRF) increases the likelihood of over-fitting the data. Thus, current and future studies could benefit from newer simultaneous multi-slice imaging protocols that allow for increased temporal resolution (e.g., TR = 200–250 ms) and improved modeling of the HRF (Thompson et al., 2014).

Conclusion

In summary, during a simple multisensory detection task, SP exhibited abnormal PSU after normal task-related activation in secondary unisensory areas, as well as abnormal task-induced deactivation in the aDMN, and the two hemodynamic abnormalities were related. Current results are consistent with the view that separate neural processes underlie the two phases of the HRF (Haigh et al., 2015; Mullinger et al., 2013; Sadaghiani et al., 2009) and that they are differentially affected in SP. Such findings do not directly contradict the large body of literature on evoked BOLD responses in SP that used a single parameter to estimate the HRF. Instead, they support caution when assuming a similar HRF shape in SP and HC which may obscure group differences related to inhibitory activation. Examination of the full time course of a deconvolved HRF provides a more thorough approach for investigating neuronal pathology in SP.

Supplementary Material

Refer to Web version on PubMed Central for supplementary material.

Acknowledgments

We would like to thank Diana South and Catherine Smith for their assistance with data collection. This work was supported by the National Institutes of Health (grant numbers NIGMS P20GM103472 (COBRE), 1R01MH101512-01A1 (R01) to A.R.M.).

Reference List

Abbott CC, Jaramillo A, Wilcox CE, Hamilton DA. Antipsychotic drug effects in schizophrenia: a review of longitudinal FMRI investigations and neural interpretations. Curr Med Chem. 2013; 20:428–437. [PubMed: 23157635]

Aboul-Fotouh S, Elgayar N. Atypical antipsychotics such as risperidone, but not paliperidone, worsen vascular endothelial function via upregulation of adhesion molecules VCAM-1, ICAM-1, and E-selectin in diabetic rats. Can J Physiol Pharmacol. 2013; 91:1119–1126. [PubMed: 24289084]

Addington D, Addington J, Maticka-Tyndale E. Assessing depression in schizophrenia: the Calgary Depression Scale. Br J Psychiatry Suppl. 1993:39–44. [PubMed: 8110442]

Attwell D, Buchan AM, Charpak S, Lauritzen M, Macvicar BA, Newman EA. Glial and neuronal control of brain blood flow. Nature. 2010; 468:232–243. [PubMed: 21068832]

Barnes TR. A rating scale for drug-induced akathisia. Br J Psychiatry. 1989; 154:672–676. [PubMed: 2574607]

Bellgowan PS, Saad ZS, Bandettini PA. Understanding neural system dynamics through task modulation and measurement of functional MRI amplitude, latency, and width. Proc Natl Acad Sci U S A. 2003; 100:1415–1419. [PubMed: 12552093]

Boorman L, Kennerley AJ, Johnston D, Jones M, Zheng Y, Redgrave P, Berwick J. Negative blood oxygen level dependence in the rat: a model for investigating the role of suppression in neurovascular coupling. J Neurosci. 2010; 30:4285–4294. [PubMed: 20335464]

Box, GEP.; Jenkins, GM.; Reinsel, GC. Time Series Analysis, Forecast and Control. Hoboken, NJ: Jon Wiley & Sons, Inc; 1994.

Braff DL, Geyer MA, Swerdlow NR. Human studies of prepulse inhibition of startle: normal subjects, patient groups, and pharmacological studies. Psychopharmacology (Berl). 2001; 156:234–258. [PubMed: 11549226]

Broyd SJ, Demanuele C, Debener S, Helps SK, James CJ, Sonuga-Barke EJ. Default-mode brain dysfunction in mental disorders: a systematic review. Neurosci Biobehav Rev. 2009; 33:279–296. [PubMed: 18824195]

Buchsbaum MS, Buchsbaum BR, Hazlett EA, Haznedar MM, Newmark R, Tang CY, Hof PR. Relative glucose metabolic rate higher in white matter in patients with schizophrenia. Am J Psychiatry. 2007; 164:1072–1081. [PubMed: 17606659]

Burock MA, Buckner RL, Woldorff MG, Rosen BR, Dale AM. Randomized event-related experimental designs allow for extremely rapid presentation rates using functional MRI. NeuroReport. 1998; 9:3735–3739. [PubMed: 9858388]

Buxton RB. Dynamic models of BOLD contrast. Neuroimage. 2012; 62:953–961. [PubMed: 22245339]

Buxton RB, Uludag K, Dubowitz DJ, Liu TT. Modeling the hemodynamic response to brain activation. Neuroimage. 2004; 23(Suppl 1):S220–S233. [PubMed: 15501093]

Buxton RB, Wong EC, Frank LR. Dynamics of blood flow and oxygenation changes during brain activation: the balloon model. Magn Reson Med. 1998; 39:855–864. [PubMed: 9621908]

Chen JJ, Pike GB. Origins of the BOLD post-stimulus undershoot. Neuroimage. 2009; 46:559–568. [PubMed: 19303450]

Cox RW. AFNI: Software for analysis and visualization of functional magnetic resonance neuroimages. Comput Biomed Res. 1996; 29:162–173. [PubMed: 8812068]

D'Esposito M, Zarahn E, Aguirre GK. Event-related functional MRI: implications for cognitive psychology. Psychol Bull. 1999; 125:155–164. [PubMed: 9990848]

De PL, Crescini A, Deste G, Fusar-Poli P, Sacchetti E, Vita A. Brain structural abnormalities at the onset of schizophrenia and bipolar disorder: a meta-analysis of controlled magnetic resonance imaging studies. Curr Pharm Des. 2012; 18:486–494. [PubMed: 22239579]

Devor A, Trevelyan A, Kleinfeld D. Is there a common origin to surround-inhibition as seen through electrical activity versus hemodynamic changes? Focus on "Duration-dependent response in SI to vibrotactile stimulation in squirrel monkey". J Neurophysiol. 2007; 97:1880–1882. [PubMed: 17215499]

Dyck M, Loughead J, Gur RC, Schneider F, Mathiak K. Hyperactivation balances sensory processing deficits during mood induction in schizophrenia. Soc Cogn Affect Neurosci. 2014; 9:167–175. [PubMed: 23051903]

Dyckman KA, Lee AK, Agam Y, Vangel M, Goff DC, Barton JJ, Manoach DS. Abnormally persistent fMRI activation during antisaccades in schizophrenia: a neural correlate of perseveration? Schizophr Res. 2011; 132:62–68. [PubMed: 21831602]

Falkenberg LE, Westerhausen R, Craven AR, Johnsen E, Kroken RA, EMLB, Specht K, Hugdahl K. Impact of glutamate levels on neuronal response and cognitive abilities in schizophrenia. Neuroimage Clin. 2014; 4:576–584. [PubMed: 24749064]

Ford JM, Johnson MB, Whitfield SL, Faustman WO, Mathalon DH. Delayed hemodynamic responses in schizophrenia. Neuroimage. 2005; 26:922–931. [PubMed: 15955502]

Forman SD, Cohen JD, Fitzgerald M, Eddy WF, Mintun MA, Noll DC. Improved assessment of significant activation in functional magnetic resonance imaging (fMRI): use of a cluster-size threshold. Magn Reson Med. 1995; 33:636–647. [PubMed: 7596267]

Fox MD, Snyder AZ, McAvoy MP, Barch DM, Raichle ME. The BOLD onset transient: identification of novel functional differences in schizophrenia. Neuroimage. 2005; 25:771–782. [PubMed: 15808978]

Fox PT, Raichle ME. Focal physiological uncoupling of cerebral blood flow and oxidative metabolism during somatosensory stimulation in human subjects. Proc Natl Acad Sci U S A. 1986; 83:1140–1144. [PubMed: 3485282]

Friedman L, Turner JA, Stern H, Mathalon DH, Trondsen LC, Potkin SG. Chronic smoking and the BOLD response to a visual activation task and a breath hold task in patients with schizophrenia and healthy controls. Neuroimage. 2008; 40:1181–1194. [PubMed: 18289881]

Fujimoto T, Takeuch K, Matsumoto T, Kamimura K, Hamada R, Nakamura K, Kato N. Abnormal glucose metabolism in the anterior cingulate cortex in patients with schizophrenia. Psychiatry Res. 2007; 154:49–58. [PubMed: 17188463]

Gaebler AJ, Mathiak K, Koten JW Jr, Konig AA, Koush Y, Weyer D, Depner C, Matentzoglu S, Edgar JC, Willmes K, Zvyagintsev M. Auditory mismatch impairments are characterized by core neural dysfunctions in schizophrenia. Brain. 2015; 138:1410–1423. [PubMed: 25743635]

Gardner DM, Murphy AL, O'Donnell H, Centorrino F, Baldessarini RJ. International consensus study of antipsychotic dosing. Am J Psychiatry. 2010; 167:686–693. [PubMed: 20360319]

Glover GH. Deconvolution of impulse response in event-related BOLD fMRI. Neuroimage. 1999; 9:416–429. [PubMed: 10191170]

Guy W. Abnormal involuntary movement scale (AIMS). ECDEU assessment manual for psychopharmacology. 1976; 338:534–537.

Haigh SM, Cooper NR, Wilkins AJ. Cortical excitability and the shape of the haemodynamic response. Neuroimage. 2015; 111:379–384. [PubMed: 25721427]

Handwerker DA, Gonzalez-Castillo J, D'Esposito M, Bandettini PA. The continuing challenge of understanding and modeling hemodynamic variation in fMRI. Neuroimage. 2012; 62:1017–1023. [PubMed: 22366081]

Harris LW, Guest PC, Wayland MT, Umrania Y, Krishnamurthy D, Rahmoune H, Bahn S. Schizophrenia: metabolic aspects of aetiology, diagnosis and future treatment strategies. Psychoneuroendocrinology. 2013; 38:752–766. [PubMed: 23084727]

Harrison BJ, Yucel M, Pujol J, Pantelis C. Task-induced deactivation of midline cortical regions in schizophrenia assessed with fMRI. Schizophr Res. 2007; 91:82–86. [PubMed: 17307337]

Harshbarger TB, Song AW. Differentiating sensitivity of post-stimulus undershoot under diffusion weighting: implication of vascular and neuronal hierarchy. PLoS ONE. 2008; 3:e2914. [PubMed: 18698432]

Heatherton TF, Kozlowski LT, Frecker RC, Fagerstrom KO. The Fagerstrom Test for Nicotine Dependence: a revision of the Fagerstrom Tolerance Questionnaire. Br J Addict. 1991; 86:1119–1127. [PubMed: 1932883]

Hua J, Stevens RD, Huang AJ, Pekar JJ, van Zijl PC. Physiological origin for the BOLD poststimulus undershoot in human brain: vascular compliance versus oxygen metabolism. J Cereb Blood Flow Metab. 2011; 31:1599–1611. [PubMed: 21468090]

Johnson JA, Zatorre RJ. Neural substrates for dividing and focusing attention between simultaneous auditory and visual events. Neuroimage. 2006; 31:1673–1681. [PubMed: 16616520]

Jurkiewicz MT, Gaetz WC, Bostan AC, Cheyne D. Post-movement beta rebound is generated in motor cortex: evidence from neuromagnetic recordings. Neuroimage. 2006; 32:1281–1289. [PubMed: 16863693]

Kay SR, Fiszbein A, Opler LA. The Positive and Negative Syndrome Scale (PANSS) for schizophrenia. Schizophrenia Bulletin. 1987; 13:261–276. [PubMed: 3616518]

Kim SG, Ogawa S. Biophysical and physiological origins of blood oxygenation level-dependent fMRI signals. J Cereb Blood Flow Metab. 2012; 32:1188–1206. [PubMed: 22395207]

Kindler J, Jann K, Homan P, Hauf M, Walther S, Strik W, Dierks T, Hubl D. Static and dynamic characteristics of cerebral blood flow during the resting state in schizophrenia. Schizophr Bull. 2015; 41:163–170. [PubMed: 24327756]

Klimesch W, Sauseng P, Hanslmayr S. EEG alpha oscillations: the inhibition-timing hypothesis. Brain Res Rev. 2007; 53:63–88. [PubMed: 16887192]

Landin-Romero R, McKenna PJ, Salgado-Pineda P, Sarro S, Aguirre C, Sarri C, Compte A, Bosque C, Blanch J, Salvador R, Pomarol-Clotet E. Failure of deactivation in the default mode network: a trait marker for schizophrenia? Psychol Med. 2015; 45:1315–1325. [PubMed: 25331916]

Lara DR. Inhibitory deficit in schizophrenia is not necessarily a GABAergic deficit. Cell Mol Neurobiol. 2002; 22:239–247. [PubMed: 12469867]

Leung JY, Barr AM, Procyshyn RM, Honer WG, Pang CC. Cardiovascular side-effects of antipsychotic drugs: the role of the autonomic nervous system. Pharmacol Ther. 2012; 135:113–122. [PubMed: 22565090]

Leung JY, Pang CC, Procyshyn RM, Barr AM. Cardiovascular effects of acute treatment with the antipsychotic drug olanzapine in rats. Vascul Pharmacol. 2014; 62:143–149. [PubMed: 24969105]

Leyba L, Mayer AR, Gollub RL, Andreasen NC, Clark VP. Smoking status as a potential confound in the BOLD response of patients with schizophrenia. Schizophr Res. 2008; 104:79–84. [PubMed: 18684594]

Liu J, Qiu M, Constable RT, Wexler BE. Does baseline cerebral blood flow affect task-related blood oxygenation level dependent response in schizophrenia? Schizophr Res. 2012; 140:143–148. [PubMed: 22789669]

Lu H, Golay X, Pekar JJ, Van Zijl PC. Sustained poststimulus elevation in cerebral oxygen utilization after vascular recovery. J Cereb Blood Flow Metab. 2004; 24:764–770. [PubMed: 15241184]

Mannell MV, Franco AR, Calhoun VD, Canive JM, Thoma RJ, Mayer AR. Resting state and task-induced deactivation: a methodological comparison in patients with schizophrenia and healthy controls. Hum Brain Mapp. 2010; 31:424–437. [PubMed: 19777578]

Mayer AR, Franco AR, Canive J, Harrington DL. The effects of stimulus modality and frequency of stimulus presentation on cross-modal distraction. Cereb Cortex. 2009; 19:993–1007. [PubMed: 18787235]

Mayer AR, Franco AR, Ling J, Canive JM. Assessment and quantification of head motion in neuropsychiatric functional imaging research as applied to schizophrenia. J Int Neuropsychol Soc. 2007; 13:839–845. [PubMed: 17697415]

Mayer AR, Ruhl D, Merideth F, Ling J, Hanlon FM, Bustillo J, Canive J. Functional imaging of the hemodynamic sensory gating response in schizophrenia. Hum Brain Mapp. 2013; 34:2302–2312. [PubMed: 22461278]

Mayer AR, Toulouse T, Klimaj S, Ling J, Pena A, Bellgowan P. Investigating the properties of the hemodynamic response function following mild traumatic brain injury. J Neurotrauma. 2014; 31:189–197. [PubMed: 23965000]

McDowell JE, Clementz BA. Behavioral and brain imaging studies of saccadic performance in schizophrenia. Biol Psychol. 2001; 57:5–22. [PubMed: 11454432]

McGregor KM, Sudhyadhom A, Nocera J, Seff A, Crosson B, Butler AJ. Reliability of negative BOLD in ipsilateral sensorimotor areas during unimanual task activity. Brain Imaging Behav. 2014; 9:245–254. [PubMed: 24788334]

McKiernan KA, Kaufman JN, Kucera-Thompson J, Binder JR. A parametric manipulation of factors affecting task-induced deactivation in functional neuroimaging. J Cogn Neurosci. 2003; 15:394–408. [PubMed: 12729491]

Mothersill O, Morris DW, Kelly S, Rose EJ, Bokde A, Reilly R, Gill M, Corvin AP, Donohoe G. Altered medial prefrontal activity during dynamic face processing in schizophrenia spectrum patients. Schizophr Res. 2014; 157:225–230. [PubMed: 24888525]

Mullinger KJ, Mayhew SD, Bagshaw AP, Bowtell R, Francis ST. Poststimulus undershoots in cerebral blood flow and BOLD fMRI responses are modulated by poststimulus neuronal activity. Proc Natl Acad Sci U S A. 2013; 110:13636–13641. [PubMed: 23898206]

Muthukumaraswamy SD, Evans CJ, Edden RA, Wise RG, Singh KD. Individual variability in the shape and amplitude of the BOLD-HRF correlates with endogenous GABAergic inhibition. Hum Brain Mapp. 2012; 33:455–465. [PubMed: 21416560]

Nygard M, Eichele T, Loberg EM, Jorgensen HA, Johnsen E, Kroken RA, Berle JO, Hugdahl K. Patients with Schizophrenia Fail to Up-Regulate Task-Positive and Down-Regulate Task-Negative Brain Networks: An fMRI Study Using an ICA Analysis Approach. Front Hum Neurosci. 2012; 6:149. [PubMed: 22666197]

Patterson TL, Goldman S, McKibbin CL, Hughs T, Jeste DV. UCSD Performance-Based Skills Assessment: development of a new measure of everyday functioning for severely mentally ill adults. Schizophr Bull. 2001; 27:235–245. [PubMed: 11354591]

Peruzzo D, Rambaldelli G, Bertoldo A, Bellani M, Cerini R, Silvia M, Pozzi MR, Tansella M, Brambilla P. The impact of schizophrenia on frontal perfusion parameters: a DSC-MRI study. J Neural Transm. 2011; 118:563–570. [PubMed: 21203783]

Petzold GC, Murthy VN. Role of astrocytes in neurovascular coupling. Neuron. 2011; 71:782–797. [PubMed: 21903073]

Poels EM, Kegeles LS, Kantrowitz JT, Javitt DC, Lieberman JA, Abi-Dargham A, Girgis RR. Glutamatergic abnormalities in schizophrenia: a review of proton MRS findings. Schizophr Res. 2014; 152:325–332. [PubMed: 24418122]

Pomarol-Clotet E, Salvador R, Sarro S, Gomar J, Vila F, Martinez A, Guerrero A, Ortiz-Gil J, Sans-Sansa B, Capdevila A, Cebamanos JM, McKenna PJ. Failure to deactivate in the prefrontal cortex

in schizophrenia: dysfunction of the default mode network? Psychol Med. 2008; 38:1185–1193. [PubMed: 18507885]

Ragland JD, Yoon J, Minzenberg MJ, Carter CS. Neuroimaging of cognitive disability in schizophrenia: search for a pathophysiological mechanism. Int Rev Psychiatry. 2007; 19:417–427. [PubMed: 17671874]

Roder CH, Hoogendam JM, van der Veen FM. FMRI, antipsychotics and schizophrenia. Influence of different antipsychotics on BOLD-signal. Curr Pharm Des. 2010; 16:2012–2025. [PubMed: 20370669]

Rowland LM, Kontson K, West J, Edden RA, Zhu H, Wijtenburg SA, Holcomb HH, Barker PB. In vivo measurements of glutamate, GABA, and NAAG in schizophrenia. Schizophr Bull. 2013; 39:1096–1104. [PubMed: 23081992]

Rowland LM, Krause BW, Wijtenburg SA, McMahon RP, Chiappelli J, Nugent KL, Nisonger SJ, Korenic SA, Kochunov P, Hong LE. Medial frontal GABA is lower in older schizophrenia: a MEGA-PRESS with macromolecule suppression study. Mol Psychiatry. 2015 Epub ahead of print.

Sadaghiani S, Ugurbil K, Uludag K. Neural activity-induced modulation of BOLD poststimulus undershoot independent of the positive signal. Magn Reson Imaging. 2009; 27:1030–1038. [PubMed: 19761930]

Schroeter ML, Kupka T, Mildner T, Uludag K, von Cramon DY. Investigating the post-stimulus undershoot of the BOLD signal--a simultaneous fMRI and fNIRS study. Neuroimage. 2006; 30:349–358. [PubMed: 16257236]

Shepherd AM, Matheson SL, Laurens KR, Carr VJ, Green MJ. Systematic meta-analysis of insula volume in schizophrenia. Biol Psychiatry. 2012; 72:775–784. [PubMed: 22621997]

Shmuel A, Augath M, Oeltermann A, Logothetis NK. Negative functional MRI response correlates with decreases in neuronal activity in monkey visual area V1. Nat Neurosci. 2006; 9:569–577. [PubMed: 16547508]

Simpson GM, Angus JW. A rating scale for extrapyramidal side effects. Acta Psychiatr Scand Suppl. 1970; 212:11–19. [PubMed: 4917967]

Stevenson CM, Brookes MJ, Morris PG. beta-Band correlates of the fMRI BOLD response. Hum Brain Mapp. 2011; 32:182–197. [PubMed: 21229612]

Talairach, J.; Tournoux, P. Co-planar Steriotaxic Atlas of the Human Brain. New York: Thieme; 1988.

Taylor SF, Tso IF. GABA abnormalities in schizophrenia: A methodological review of in vivo studies. Schizophr Res. 2014; 167:84–90. [PubMed: 25458856]

Thompson SK, Engel SA, Olman CA. Larger neural responses produce BOLD signals that begin earlier in time. Front Neurosci. 2014; 8:159. [PubMed: 24971051]

Van Snellenberg JX, Torres IJ, Thornton AE. Functional neuroimaging of working memory in schizophrenia: task performance as a moderating variable. Neuropsychology. 2006; 20:497. [PubMed: 16938013]

van Zijl PC, Hua J, Lu H. The BOLD post-stimulus undershoot, one of the most debated issues in fMRI. Neuroimage. 2012; 62:1092–1102. [PubMed: 22248572]

Vita A, De PL, Deste G, Sacchetti E. Progressive loss of cortical gray matter in schizophrenia: a meta-analysis and meta-regression of longitudinal MRI studies. Transl Psychiatry. 2012; 2:e190. [PubMed: 23168990]

Wechsler, D. Wechsler Test of Adult Reading: WTAR. Psychological Corporation; 2001.

Zhu J, Zhuo C, Qin W, Xu Y, Xu L, Liu X, Yu C. Altered resting-state cerebral blood flow and its connectivity in schizophrenia. J Psychiatr Res. 2015; 63:28–35. [PubMed: 25812945]

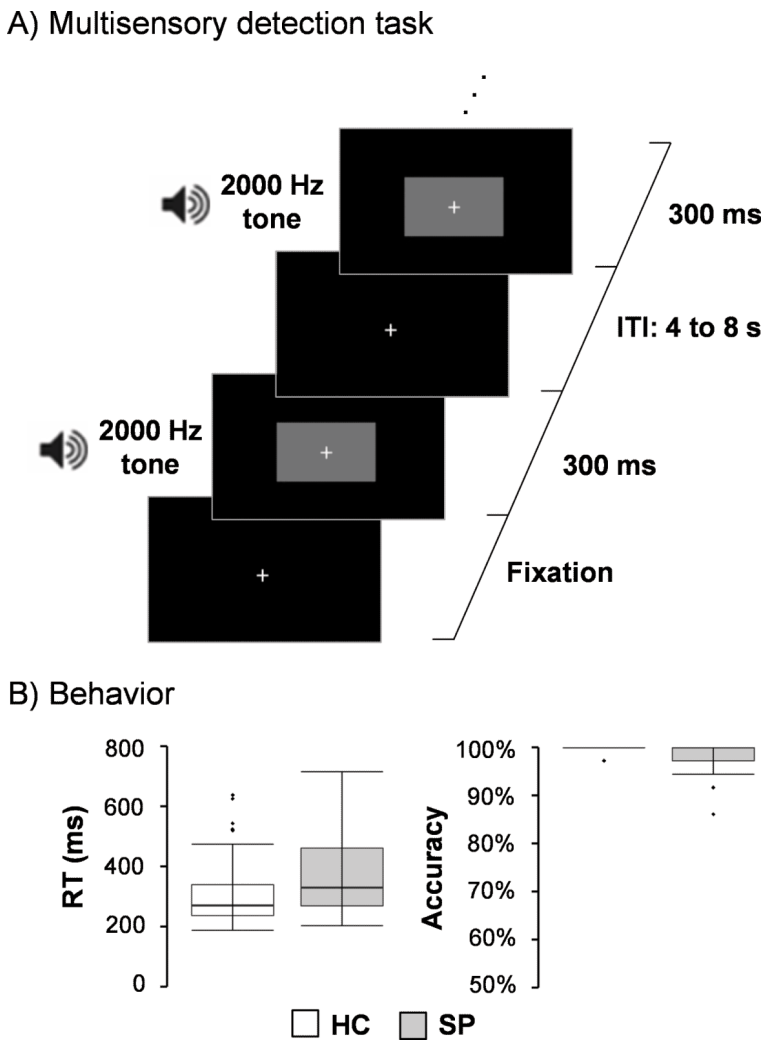

Figure 1.

Panel A presents a diagrammatic representation of the multisensory detection task, beginning with fixation. The target stimuli consisted of a blue rectangle (displayed as gray in this figure) and a 2000 Hz tone simultaneously presented for 300 ms. Participants responded with a button press. The baseline consisted of a white visual fixation cross on a black background (ITI: 4 to 8 seconds). Panel B depicts box-and-whisker plots for reaction times (RT) and accuracy for healthy controls (HC) and patients with schizophrenia (SP).

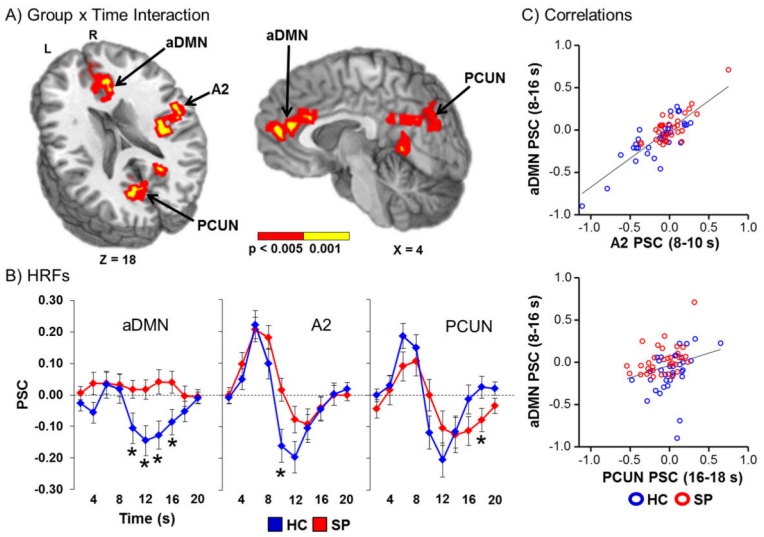

Figure 2.

Panel A displays the regions of the brain showing a significant Group x Time (0 to 20 s post-stimulus onset) interaction (red: significant at $p < 0.005$; yellow: $p < 0.001$). Locations of the sagittal (X) and axial (Z) slices are given according to the Talairach atlas for the left (L) and right (R) hemispheres. These areas included regions of the anterior default-mode network (aDMN); right secondary auditory cortex (A2); and the bilateral precuneus (PCUN). Panel B displays the percent signal change (PSC) by group (healthy controls (HC) shown in blue and patients with schizophrenia (SP) in red) for the entire HRF. Time-points (sampled at 2 s intervals) exhibiting significant differences during simple effect testing are indicated with an asterisk (*). Panel C illustrates the significant relationships between aDMN activity with other regions (A2 and PCUN) exhibiting a significant interaction effect.

Table I

Summary of participant demographic and clinical measures.

	SP		HC		Statistics	
	Mean	**SD**	**Mean**	**SD**	***p* value**	**Cohen's D**
Demographics						
Gender (Females/Males)	6/27		6/28			
Age (years)	38.09	13.66	37.50	13.35	$p = .858$	0.04
Education Level	12.61	1.77	12.74	1.83	$p = .770$	−0.07
Clinical Measures						
WTAR	55.08	12.96	58.14	7.36	$p = .253$	−0.29
Age of onset (years)	22.50	7.45				
PANSS Positive	14.76	4.32				
PANSS Negative	15.70	5.28				
PANSS Total	58.67	13.71				
UPSA-2 Total	98.91	12.46				
Calgary Depression Scale	3.30	3.87				
FTND	0.55	1.00				
Olanzapine equivalent	11.77	7.48				
SAS	1.30	1.59				
AIMS	1.18	2.16				
BAS	0.24	0.50				

Notes: SP = Patients with schizophrenia; HC = Healthy controls; SD = standard deviation; WTAR = Wechsler Test of Adult Reading; PANSS = Positive and Negative Syndrome Scale; UPSA-2 = UCSD Performance Based Skills Assessment, Second Version; FTND = Fagerstrom Test for Nicotine Dependence; SAS = Simpson Angus Scale; AIMS = Abnormal Involuntary Movements Scale; BAS = Barnes Akathisia Scale. Education level was determined based on number of years in school.